Jurnal Teknologi Reaktor Nuklir

Tri Dasa Mega

Journal homepage: https://ejurnal.brin.go.id/tridam

Boron Neutron Capture Therapy (BNCT) Dose Optimization for Ovarian Cancer Oligometastatic Using Particle and Heavy Ion Transport Code System (PHITS) v3.35

Al Fiyatuz Zuhroh[1*], Mokhamad Tirono[1], Yohannes Sardjono[2], Gede Sutresna Wijaya[2], Isman Mulyadi Triatmoko[2], Fendi Nugroho[2],

[1]Department of Physics, Faculty of Science and Technology, Maulana Malik Ibrahim State Islamic University, Malang, Indonesia
[2]Research Center for Safety, Meteorology and Nuclear Quality Technology, Research Organization for Nuclear Energy, National Research and Innovation Agency (BRIN), Yogyakarta, Indonesia

ARTICLE INFO

Article history:

Received: August 22, 2025
Received in revised form: Oct. 10, 2025
Accepted: November 26, 2025

Keywords:

BNCT
Dosimetry
Ovarian Cancer Oligometastases
PHITS

A B S T R A C T

In Indonesia, ovarian cancer ranks third among cancer-related deaths, with a poor prognosis largely due to late-stage diagnosis and limited treatment efficacy. Boron Neutron Capture Therapy (BNCT) has emerged as a promising alternative, offering selective tumor cell destruction through boron-10–mediated nuclear reactions. This study employed PHITS v3.35 to simulate BNCT in a case of oligometastatic ovarian cancer with para-aortic lymph node involvement (FIGO IIIC). The neutron source was a 30 MeV cyclotron. Simulations were conducted with two irradiation directions, posterior–anterior (PA) and left lateral (LLAT), and three boron concentrations of 100, 120, and 145 µg/g. The PA direction provided a more focused dose distribution to the tumor target and a shorter irradiation time compared to LLAT. The results indicated that the posterior–anterior (PA) beam configuration provided a more favorable balance between tumor dose coverage, irradiation time, and organ-at-risk (OAR) sparing compared to the lateral approach. These findings suggest that PA irradiation with 120 µg/g boron concentration may represent a promising option in BNCT planning for ovarian cancer. However, as this work is based on simulation in an idealized phantom, further experimental and clinical validation is required before clinical application can be considered.

1. INTRODUCTION

Cancer is the second leading cause of death worldwide, with an estimated 9.6 million deaths annually [1]. According to GLOBOCAN 2020, there were 19.3 million new cancer cases globally, with ovarian cancer accounting for about 324,603 new cases and 206,956 deaths [2]. In Indonesia, ovarian cancer ranks third among cancer-related deaths [2][3]. The high mortality rate is mainly due to the difficulty of early-stage detection, as most cases are diagnosed at an advanced stage, which often requires intensive treatment and leads to a poor prognosis [4][5].

In recent years, immunotherapy has been considered a potential treatment for ovarian cancer [6], particularly through the use of immune checkpoint inhibitors such as anti-PD-1, anti-PD-L1, and anti-CTLA-4. However, clinical outcomes are modest, especially in platinum-resistant cases, with

* Corresponding author. Tel./Fax.
E-mail: alfiazuhro@gmail.com
DOI:10.55981.tdm.2025.13334

response rates often below 10% [7]. This limited efficacy is largely due to the immunosuppressive tumor microenvironment of ovarian cancer, characterized by low infiltration of cytotoxic CD8+ T cells and a high presence of regulatory T cells and myeloid-derived suppressor cells. Furthermore, immunotherapy often causes immune-related side effects and requires tumor-specific biomarkers, making its application inconsistent across patient populations. Given these limitations, alternative treatment modalities that do not rely on immune system activation are urgently needed [7]. Among radiation-based strategies, stereotactic body radiation therapy (SBRT) has been explored as a precise modality targeting specific anatomical sites. However, its efficacy is limited by toxicity in surrounding healthy tissue [8]. A more promising approach is Boron Neutron Capture Therapy (BNCT), a binary radiation technique that selectively targets boron-10-enriched tumor cells, inducing lethal damage through nuclear reactions while sparing nearby healthy tissue [9]. Although BNCT has shown promise in several malignancies, its application in ovarian cancer remains largely unexplored.

BNCT has been widely investigated in recurrent head and neck cancers, with several studies reporting favorable outcomes, including tumor regression, response rates of up to 76%, and median survival extending to nearly 24 months [10]. However, these studies were constrained by small patient numbers, prolonged irradiation times, radiation-induced toxicities such as oral mucositis and dermatitis, and inter-patient variability in boron uptake, which limit their broader clinical applicability [11]. Moreover, the application of BNCT in ovarian cancer has not yet been systematically studied. To address these limitations, the present study simulates a case of ovarian cancer with solitary metastatic oligorecurrence in a para-aortic lymph node, classified as FIGO stage IIIC [12]. The objective is to determine the therapeutically effective dose of BNCT and to identify the optimal irradiation direction and exposure time using PHITS v3.35.

2. THEORY

Boron Neutron Capture Therapy (BNCT) is a therapeutic modality that utilizes the isotope 10B, which is absorbed by cancerous cells. Subsequently, the cells are exposed to thermal neutrons, resulting in the emission of high-energy particles (α-particles and lithium-7), thereby eradicating the cancerous cells without compromising the surrounding healthy tissue [13]. As stated in reference 6, the lowest LET (linear energy transfer) of an alpha particle is 164 keV/μm, with a range of 9 μm, and the LET of 7Li is 151 keV/μm, with a range of 5 μm [14]. In the event that reaction 10B(n, a)Li manifests exclusively within a neoplastic cell, it is imperative to devise a selective boron-bearing agent. Figure 1 is a presentation of the BNCT therapeutic protocol [15].

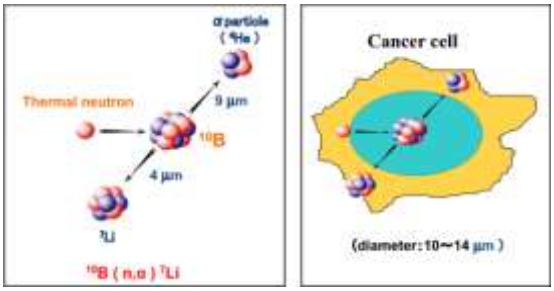

Figure 1. (A) The 10B(n,α)7 Li capture reaction results in the production of high linear energy transfer (LET) alpha particles (stripped of 4 He nuclei) and retreating lithium-7 (7 Li) atoms. (B) A sufficient amount of 10B must be selectively delivered to the tumor, ranging from ~20 to 50 μg/g

Two agents are utilized in this therapeutic modality: sodium borocaptate (BSH) and boronophenylalanine (BPA) [16]. The two agents responsible for transporting boron have distinct functions. BSH accumulates in the space between tumor cells, while BPA can enter tumor cells directly via amino acid transport [13]. Subsequent to the accumulation of boron-10 within the cancerous cell, neutron bombardment is initiated, with the neutrons emanating from the accelerator.

The generation of neutrons in BNCT does not exclusively rely on accelerators; reprocessing facilities are also utilized. Nevertheless, the selection of this accelerator was made on the basis that it is more feasible to install it in a hospital setting [17]. It is evident that the output of this accelerator is equivalent to that of a reactor. The accelerator utilized in the BNCT therapeutic modality is based on a cyclotron manufactured by Sumitomo Heavy Industries (SHI), operating at an energy level of 30 MeV [18]. Protons produced from the accelerator are fired at the target metal 9Be, which reacts to release 9Be(n,p)10B [19]. This reactor, however, emits neutrons with significant energy, which is ~28.1 MeV. This neutron energy is included in the fast neutron category [20]. It is imperative to utilize the Beam Shaping Assembly (BSA) [21], which comprises a moderator, reflector, filter, gamma shielding, and aperture. Each component fulfills a

distinct function, namely the moderation of neutron output to produce thermal (>0.5 eV) and epithermal (0.5 eV-10 keV) neutrons [22]. The calculation of the output, encompassing the dosage and the neutron flux, as well as the dosage of boron-10 within the body, is performed utilizing the PHITS simulation.

In order to execute a simulation, the PHITS (Particle on Heavy Ion Transport Code System) software is employed. This software is utilized in the BNCT (Boron Neutron Capture Therapy) therapy, and it is the most recent version that has been released by JAEA (Japan Atomic Energy Agency) [23]. The purpose of employing this software is to enhance the validity and precision of the simulation [24]. PHITS is a code based on the Monte Carlo method that is generally available for the purpose of simulating radiation transport. This code has the capacity to model the movement of a variety of particles, including ions, with energies up to 1 TeV per nucleon. PHITS has been demonstrated to be a reliable tool for calculating the mean dose and determining the 3D dose distribution [25]. It has been shown to provide highly precise estimates of the dose absorbed by the patient, with a corresponding accuracy in dose projection. PHITS is the most accurate component because it relies on simulations of proton and ion transport via ATIMA (Atomic Interaction with Matter) and electron and positron transport using EGS5 (Electron Gamma Shower Ver.5), both of which play a crucial role [26].

To our knowledge, this is among the first simulation studies of BNCT for ovarian cancer, employing the PHITS version 3.35 software. Previous studies on BNCT employed simulation equipment that yielded protracted exposure times. Prolonged procedures have the potential to induce physical and psychological discomfort in patients, including fatigue. Furthermore, extended periods of ultraviolet (UV) exposure can elevate the probability of dermal damage, including skin cancer. An extended duration of the treatment can result in a reduction in its effectiveness. Consequently, this issue will serve as a reference for future researchers who wish to analyze the effectiveness of BNCT in treating ovarian cancer. This analysis will employ two different types of radiation therapy: PA and LLAT. The objective is to determine the most effective direction for delivering the radiation dose to the cancerous tissue while minimizing radiation exposure to healthy organs. The program simulation utilized is PHITS version 3.35, a selection that was made on the basis of its proven superiority in terms of the swiftness with which it initiates operations and the precision of its computations.

3. METHODOLOGY

The following methodology was employed to support the research study's simulation:

1. The portable computer with the following specifications: an AMD A9 7th GEN processor, 8 GB of RAM, and a Windows 10 Home 64-bit operating system.
2. The software in question is PHITS version 3.35
3. Microsoft Word 2021
4. Microsoft Excel 2021
5. Google Colaboratory With Python 3.0
6. Notepad ++

3.1 Patient Model

Prior to undergoing therapy, the patient's position is simulated using the PHITS software with a geometrical model based on the Oak Ridge National Laboratory (ORNL) adult female phantom model and body composition data from Report 145 of the International Commission on Radiological Protection (ICRP). The program MCNP-4B was utilized for its formulation, and subsequently, it was incorporated as the input parameter within the PHITS simulation [27]. The utilization of codes is meticulously tailored to align with the specific requirements of the research model. The organs utilized in the present study encompass the lymph, kidney, small intestine, large intestine, liver, spine, and skin [28].

The ovarium cancer model employed in this study is based on a case of ovarian cancer affecting a 74-year-old female patient with a history of stage IIB serous papillary ovarian cancer [29]. At the time of diagnosis, a computed tomography (CT) scan revealed a limited number of metastases in the pelvis, with no evidence of nodal involvement. Approximately four years following the initial biopsy, subsequent imaging revealed a solitary, enlarged lymph node in the para-aortic region, raising suspicion for malignancy. Within the framework of the BNCT planning system, three distinct target volumes are identified. The Gross Tumor Volume (GTV), Clinical Tumor Volume (CTV), and Planning Tumor Volume (PTV) were measured at 2.52 cc, 6.95 cc, and 28.94 cc, respectively [30]. As shown in Figure 3, the visual depiction of the two-dimensional geometry of the ovary can be observed.

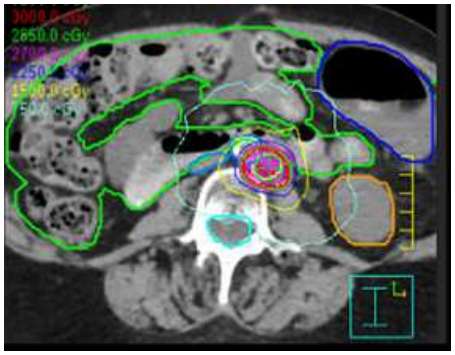

Figure 2. Transverse CT scan image in patient with ovarian cancer

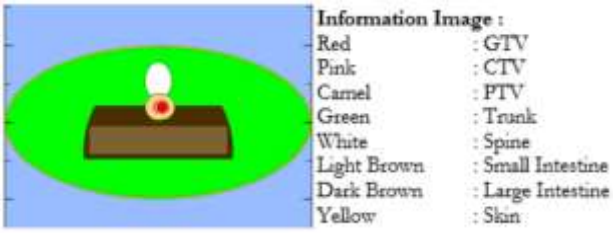

Figure 3. Geometric image of ovarian cancer and organs at risk

3.2 Neutron Source

The present study utilizes a neutron source, namely a cyclotron accelerator manufactured by Sumitomo Heavy Industries. This accelerator generates a beam of protons with an energy level of 30 MeV, as documented in the BNCT reference compendium [31]. As depicted in Figure 4 of this study, the BSA collometer was derived from the optimized replication performed by I Made Ardhana [32].

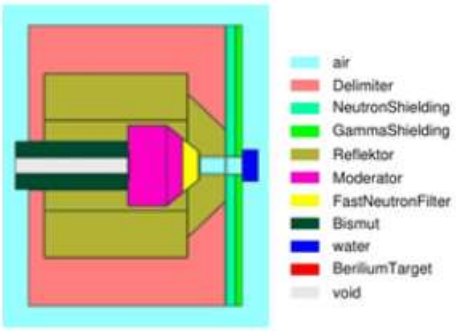

Figure 4. Beam shaping assembly design

As shown in Table 1, the parameters of neutron flux and dose rate are in accordance with the recommendations provided by the International Atomic Energy Agency (IAEA).

Table 1. Parameters of neutron flux and dose rate

Parameter	IAEA Recommendations	Result
Epithermal Neutron Flux (n/cm^2 s)	>1.0 × 10^9	1.1316 x 10^9
Fast Neutron Dose Rate/Epithermal Neutron Flux (Gy cm^2 /n)	<2.0 × 10^{-13}	6.35 x 10^{-14}
Gamma Dose Rate/Ephitermal Neutron Flux (Gy cm^2 /s)	<2.0 × 10^{-13}	8.35 x 10^{-14}
The ratio of Thermal and Epithermal Neutron Flux ($\phi th/\phi_{epi}$)	<0.05	0.0252
The Ratio of Neutron Current and Neutron Flux (J/ϕ_{epi})	>0.7	0.785

3.3 Dosimetry

The dosimetry of BNCT is comprised of the following components: gamma dose, boron dose, neutron dose, and proton dose [33]. The values of the dose rates for the four components were obtained from the PHITS output and subsequently processed using Microsoft Excel to calculate the duration of exposure and the equivalent dose rate [34].

a) The calculation of the total dose rate is derived from the multiplication of the individual dose rate for each source by the efficacy factor of the radiation source, as illustrated in Table 2. The total dosage can be calculated using the formula given in equation 1.

$$E\dot{D}\left(\frac{G_y}{s}\right) = (CBE_B\ x\ \dot{D}_B) + (RBE_n\ x\ \dot{D}_N) + (RBE_H\ x\ \dot{D}_H) + (\dot{W}_y x \dot{D}_y)$$

The subscripts D, B, N, and H represent, respectively, the dose of alpha particles, the dose of neutron particles, the dose of proton particles, and the dose of gamma-rays [35]. The values of CBE and RBE used can be found in Table 2 [36].

Table 2. CBE and RBE values of each component

Tissue Type	CBE	RBE_N	RBE_H	RBE_Y
Tumour	3.8	2.9	2.4	1
Skin	2.5	2.9	2.4	1
Bone	1	2.9	2.4	1
Soft Tissue	1.34	2.9	2.4	1

b) Irradiation Time

The duration of the irradiation process is a critical factor in the BNCT therapeutic protocol, as it determines the efficacy of the treatment in eradicating cancerous cells. The time required for the achievement of minimum effective dose for the gross target volume (GTV) can be calculated. The calculation of the time of irradiation is performed using the following equation [37].

$$irradiation\ time\ (s) = \frac{dosis\ minimum\ (Gy)}{\dot{D}_{total}\ \frac{(Gy)}{s}}$$

The total dose is defined as the total dosage administered to a cancer patient.

c) Equivalent Dose

Subsequent to the exposure period, the equivalent dose can be calculated using the actual tissue and cancerous tissue samples. The equivalent dose is employed to ascertain the extent of the damage to the healthy tissue in the vicinity of the tumor. The calculation of the dose absorbed by each organ can be performed using the following equation:

$$D_{eq}OAR\ (Gy) = \left(E\dot{D}\ OAR\ \frac{Gy}{s}\right) x\ irradiation\ time(s)$$

The distribution of the dosage and the timing of the exposure to BNCT were conducted using PHITS and calculated with concentrations of 100 µg/g, 120 µg/g, and 145 µg/g, respectively.

3.4 Monte Carlo Simulation Parameters

BNCT dose simulations in this study were performed using the Monte Carlo engine of PHITS v3.35. For each irradiation geometry, PA and LLAT, 2×10^8 particle histories were simulated to balance statistical reliability with the available computational resources [38]. The computation time for each individual case was approximately 22 hours and 20 minutes on a laptop computer (CPU: AMD A9 7th Gen processor, 8 GB RAM, Windows 10).

The statistical uncertainty of the simulations was quantified using the 1σ relative error reported by PHITS. In most tallies, the relative error ranged between 3% and 10%, with occasional higher values up to ~60% in low-flux regions or tallies with very small statistical weight, similar to the ranges reported in previous Monte Carlo dose evaluations [39]. For dose rate components, the relative error was consistently lower, ranging from 3% to 20%. Importantly, in the tumor target volumes (GTV and CTV), the relative error remained within acceptable limits (<5%), which is considered clinically acceptable in BNCT simulation studies [36].

The higher uncertainties observed in some neutron components reflect a limitation of the computational hardware, which prevented increasing the number of simulated particle histories beyond 2×10^8. This constraint should be regarded as a limitation of the current work, and future studies with higher-performance computing resources may further reduce statistical uncertainties [40].

4. RESULTS AND DISCUSSION

4.1 Irradiation Geometry

In this study, the direction of irradiation was carried out in two different directions, namely posterior-anterior (PA) and left lateral (LLAT), to obtain the optimal irradiation direction in ovarian cancer treatment using BNCT. Irradiation from the PA direction means that the irradiation is given from the back of the patient's body to the front, directly targeting the cancer area from the posterior side. While the LLAT direction is radiation given from the left side of the patient's body, aiming at the cancer area from the left lateral side. Figures 5 and 6 show the design of the BSA collimator direction using the ORNL phantom for the PA and LLAT irradiation directions, which show the differences in irradiation approaches and how each direction can affect the distribution of radiation doses in ovarian cancer tissue.

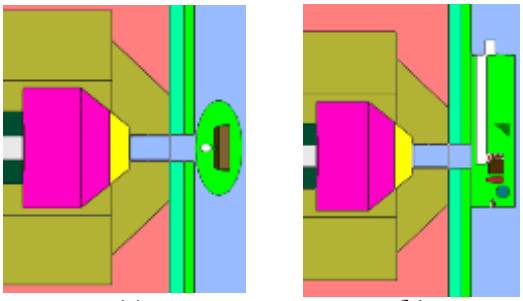

(a) (b)

Figure 5. Visualization of PA radiation in (a) axial (b) sagital section

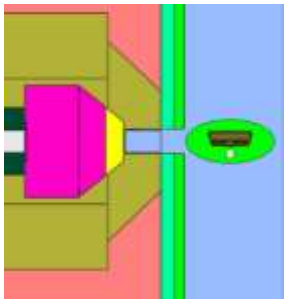

Figure 6. Visualization of LLAT radiation in axial section

In the PA configuration (Figure 5), the BSA system is positioned parallel to the longitudinal axis of the body from the posterior direction, so that the thermal and epithermal neutron beams are directed from the back of the body towards the anterior. This orientation aims to reach the ovarian tumor target located in the posterior pelvic cavity, with a more direct neutron path and potentially reducing dose exposure to anterior organs such as the kidney and small intestine.

In contrast, the LLAT configuration (Figure 6) places the BSA on the left side of the phantom, so that irradiation is delivered from the left lateral side toward the right side of the body. This approach takes advantage of the lateral geometry to penetrate soft tissue horizontally toward the tumor target. The LLAT direction has the potential to produce a more homogeneous dose distribution to lateral or more diffused lesions, but requires further evaluation of exposure to critical organs on the side of the trajectory, such as the descending colon or left kidney.

To find the ideal irradiation direction for the effectiveness of therapy and protection of healthy tissue, changes in the irradiation direction will affect the distribution of neutron flux, dose contribution from the 10B(n,α)7Li reaction, and the total dose received by both targets and organs at risk (OAR). The simulation results show that the most effective irradiation direction is from the PA angle because the distance from the aperture to the cancer in the PA irradiation direction is only 7.3 cm compared to LLAT, whose aperture depth to the cancer is 18.8 cm. Because the depth of the cancer from the PA irradiation direction is closer to the BSA, the thermal and epithermal neutron fluxes that reach the cancer are greater because the body tissue experiences little attenuation. As a result, the ^{10}B(n,α)7Li reaction becomes more effective in increasing the dose in the GTV.

4.2 Dose Rate

To prove the effectiveness and safety of BNCT therapy, an analysis of the dose rate received by the target tumor and surrounding healthy organs was performed. Dose rate is an important parameter in radiotherapy because it determines the rate of dose accumulation in the target tissue and allows for more accurate estimation of the irradiation time. In this simulation, the total dose rate is calculated based on four main components, namely: boron dose, neutron dose, proton dose, and photon dose.

The analysis was performed for two irradiation directions, posterior-anterior (PA) and left lateral (LLAT), with three variations of boron concentration: 100, 120, and 145 μg/g. The ratio of boron concentration between cancer and healthy organs is 10:1 [37]. This assumption follows common practice in BNCT treatment planning studies, where T/N ratios greater than 3:1 are generally considered sufficient for therapeutic effect, and ratios approaching 10:1 have been reported in preclinical and clinical settings using BPA or BSH [41]. Since specific pharmacokinetic data for ovarian cancer are limited, the 10:1 ratio was selected here as a simplified assumption to enable dose comparison between irradiation geometries. The distribution of dose rates to various organs is shown in the following graph, which will be the basis for determining the optimal direction and concentration in BNCT therapy for oligometastatic ovarian cancer.

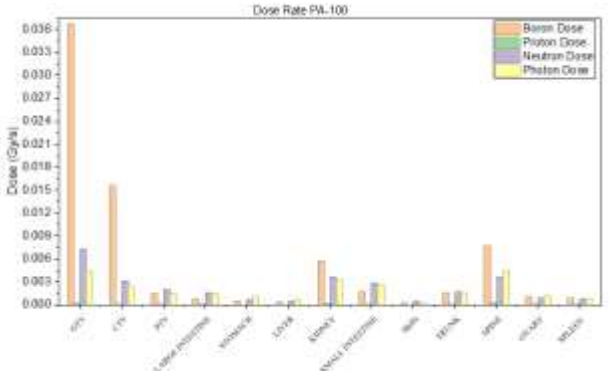

Figure 7. Dose rate distribution from PA-100 μg/g

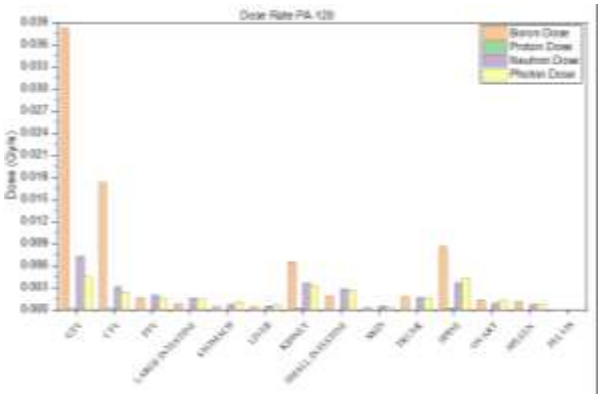

Figure 8. Dose rate distribution from PA-120 μg/g

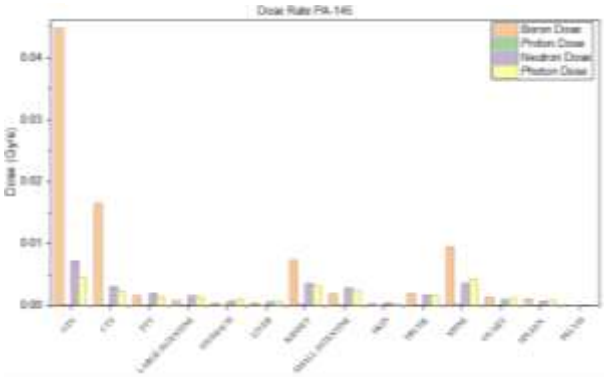

Figure 9. *Dose rate distribution from PA-145 μg/g*

The PHITS simulation results show that the posterior-anterior (PA) irradiation direction provides a more focused dose rate distribution on the target volume (GTV and CTV) compared to the left lateral (LLAT) direction. Increasing the boron concentration from 100 µg/g to 145 µg/g consistently increases the dose rate on the GTV, both in the PA and LLAT irradiation directions. However, the dose increase also occurs in healthy organs (organs at risk), especially at a concentration of 145 µg/g.

After analyzing the dose rate in the posterior-anterior (PA) irradiation direction, simulation and evaluation were carried out for the left lateral (LLAT) irradiation direction. The LLAT direction simulates neutron exposure from the left side of the patient's body, which allows lateral radiation distribution to the target. Similar to the PA configuration, the analysis was carried out with three variations of boron concentration (100, 120, and 145 µg/g) with a tumor boron ratio to healthy tissue of 10:1. The graph below shows the distribution of dose rates received by the tumor target and healthy organs in the LLAT irradiation direction.

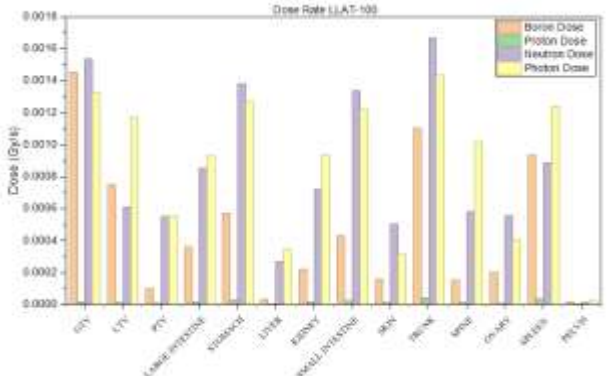

Figure 11. Dose rate distribution from LLAT-100 µg/g

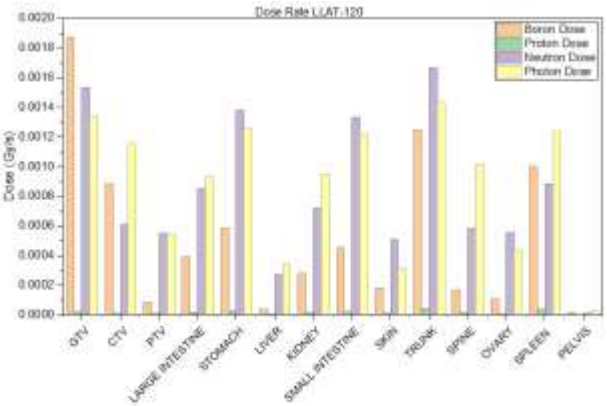

Figure 12. Dose rate distribution from LLAT-120 µg/g

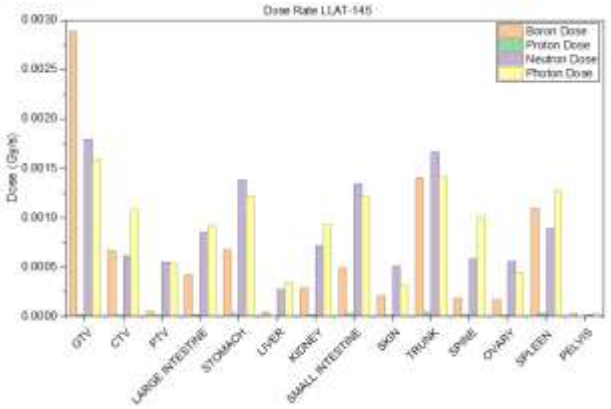

Figure 10. Dose rate distribution from LLAT-145 µg/g

In the PA direction, a concentration of 120 µg/g provides a high dose rate to the GTV (3.7 x 10^{-2} Gy/s) with a dose distribution that is still relatively safe to the surrounding organs. The dominant contribution comes from the boron component, followed by neutrons and nitrogen. Meanwhile, in the LLAT direction, the dose distribution tends to be more diffused and less selective, with OARs such as the trunk, spleen, and kidney receiving relatively high doses, even approaching or exceeding the GTV dose, especially at a concentration of 145 µg/g.

4.3 Total Dose

After analyzing the dose rate for each direction and the variation of boron concentration, the next step is to calculate the total dose received by the target organ and healthy organs. The total dose is the accumulation of the contribution of each radiation component (boron, neutrons, protons, and photons) during the irradiation time. The formula for calculating the total dose is in point 3.3(a). The following graph shows the distribution of the total dose received by healthy organs and tumor targets.

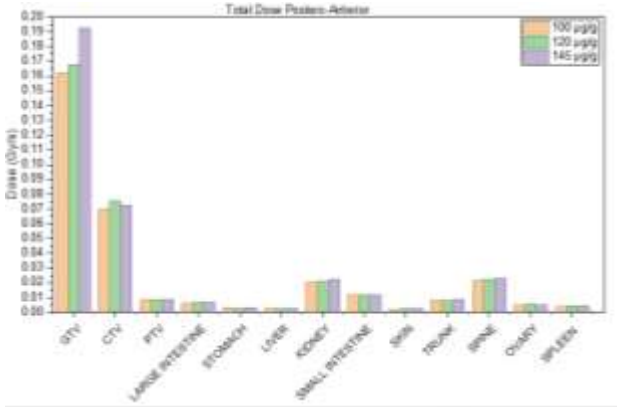

***Figure 13**. Total dose distribution from PA irradiation*

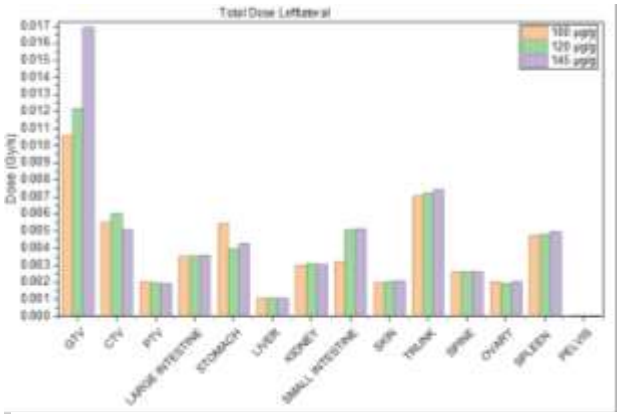

Figure 14. Total dose distribution from LLAT irradiation

Both total dose graphs show the results of the accumulated dose received by the target organs (GTV, CTV, PTV) and the surrounding healthy organs (OAR) in two different irradiation directions, namely posterior-anterior (PA) and left lateral (LLAT), each with three variations of boron concentration: 100, 120, and 145 µg/g. This analysis was conducted to assess the effectiveness of the irradiation direction in delivering doses selectively to the tumor area, while evaluating the risk of exposure to surrounding organs.

In the PA direction, the dose received by the GTV was much higher than in the LLAT direction for all concentration variations. Meanwhile, the dose distribution to healthy organs such as the kidney, spleen, intestines, and trunk was relatively lower in the PA direction compared to LLAT. In the LLAT direction, the dose increase not only occurred in the GTV, but also spread to several OARs, such as the trunk and spleen, which received doses approaching or even exceeding the CTV dose. Figures 13 and 14 show that LLAT has limitations in focusing energy only on the target, and has the potential to increase unnecessary exposure to healthy tissue.

4.4 Equivalent Dose

In addition to evaluating the rate and total dose, it is also important to know the biological impact of radiation on healthy organs (organs at risk) located around the tumor target. Therefore, the equivalent dose was calculated for each OAR based on the total dose received from the PHITS simulation.

The equivalent dose reflects the biological effects of various types of radiation, such as neutrons, protons (nitrogen reactions), and boron reaction particles, on living tissue. This value is obtained by multiplying each dose component by the appropriate RBE or CBE factor, thus providing an overview of the risk of tissue damage.

In this study, the equivalent dose was only calculated for healthy organs, with the aim of ensuring that the simulated BNCT therapy did not exceed the biological tolerance limit of the OAR.

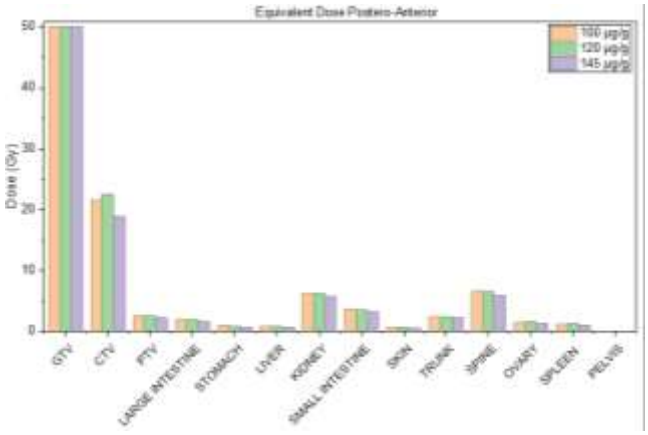

Figure 15. Equivalent dose distribution for organs at risk from PA irradiation

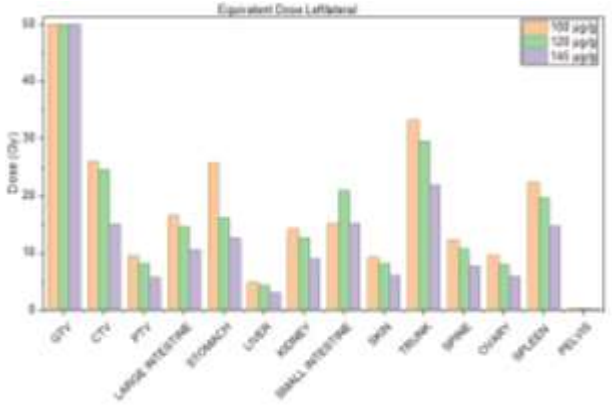

Figure 16. Equivalent dose distribution for organs at risk from LLAT irradiation

The two graphs above show equivalent dose (Gy) graphs that show how much biological effect of radiation is received by healthy organs (OAR) in two directions of radiation: posterior-anterior (PA) and left lateral (LLAT), each for three variations of boron concentration: 100, 120, and 145 µg/g.

The PA irradiation direction shows lower equivalent doses for all OARs compared to LLAT. The kidney, small intestine, and spine are the organs that receive the highest doses, but the values are still below the maximum dose found in LLAT. This graph reinforces that the alignment from the posterior direction tends to be smoother towards the tumor target.

In the LLAT direction, it can be seen that the OARs receive relatively high equivalent doses. The spleen receives the highest dose, with values reaching >20 Gy-Eq for a boron concentration of 100 µg/g, and slightly decreasing at a concentration of 145 µg/g. Figures 15 and 16 show that increasing boron concentrations is not always accompanied by increasing equivalent doses, which may be due to the proportion of boron remaining low in healthy tissue or the distribution of neutron particles spreading

laterally. Doses to organs such as the liver, skin, and ovaries tend to be lower than those to the stomach and spleen. Below is the dose tolerance that has been compared with the simulation results in order to find out which OAR has a dose that exceeds the threshold dose.

Table 3. OARs dose, direction of irradiation, and irradiation time

OAR	Irradiation Technique	PA	LLAT
	irradiation Time	297.82 second	4098.65 second
	Dose Tolerance (Gy)	Equivalent Dose (Gy)	
Skin	2	0.65	8.26
Kidney	23	6.28	12.7
Liver	30	0.78	4.33
Stomach	50	0.79	16.1
Large Intestine	40	1.94	14.5
Small Intestine	45	3.60	20.9
Spine	30	6.62	10.8
Spleen	30	1.25	19.7
Ovary	2	1.59	7.94

Comparison of equivalent doses to biological tolerance limits in healthy organs (OARs) was performed for two radiation directions, namely posterior-anterior (PA) and left lateral (LLAT). The aim is to determine the safety level of radiation exposure to normal tissue during BNCT therapy.

In the PA direction with an irradiation time of 297.82 seconds, all OARs showed equivalent doses that were below their respective tolerance limits, indicating that this direction is relatively safe. For example, the kidney received 6.28 Gy from a tolerance of 23 Gy, the spine 6.62 Gy from 30 Gy, and the ovary 1.59 Gy from 2 Gy. Although the value in the ovary is close to the tolerance threshold, the dose is still within acceptable limits. Other organs such as the liver, stomach, and large and small intestines received even lower doses, so the risk of biological complications in the PA direction is minimal.

In contrast, the LLAT direction requires a much longer irradiation time, namely 4098.65 seconds and causes a significant increase in equivalent doses in almost all OARs. Some organs experienced exposure that even exceeded the safe limit, such as the skin (8.26 Gy of the 2 Gy limit) and the ovaries (7.94 Gy of the 2 Gy limit), indicating a potential risk of toxicity that requires careful consideration. In addition, the kidneys and spleen also received quite high doses, although still within the absolute tolerance limit. This condition indicates that LLAT is at higher risk in terms of exposure to non-target organs.

Thus, it can be concluded that the PA direction is superior to protection against OARs, because it provides a lower dose with a much shorter irradiation time. Therefore, the PA direction is recommended in BNCT therapy for ovarian cancer, because it provides a balance between therapeutic efficacy and biological safety.

4.5 Irradiation Time

After the dose value on the target organ and healthy organs is known, the next step is to calculate the irradiation time needed to achieve the therapeutic dose on the main target, namely the Gross Tumor Volume (GTV). The irradiation time is calculated based on the amount of equivalent dose to be achieved and the total dose rate obtained from the simulation. This calculation is important because in BNCT practice, the irradiation time must be sufficient to produce a therapeutic effect, but it is still maintained so that exposure to healthy organs (OAR) does not exceed the tolerance limit.

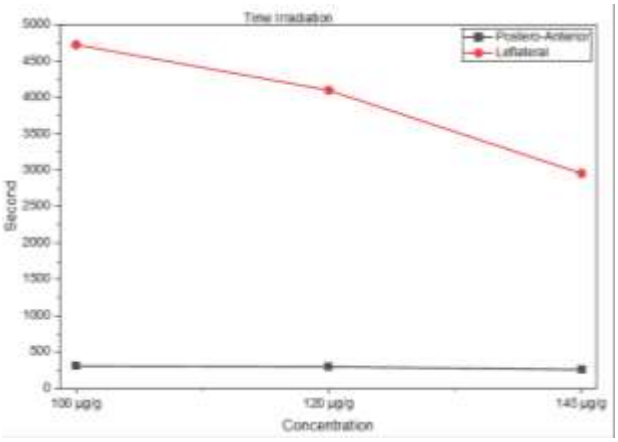

Figure 17. Irradiation time from PA and Left Lateral directions

Figure 17 above shows the irradiation time (in seconds) required to achieve an equivalent dose of 50 Gy on the GTV, for two main irradiation directions, namely posterior-anterior (PA) and left lateral (LLAT), with three variations of boron concentration: 100, 120, and 145 µg/g.

The calculation results show that the PA direction requires a much shorter irradiation time than LLAT at all boron concentrations. At a concentration of 100 µg/g, the PA irradiation time is only 308.48 seconds, while LLAT requires 4726.13 seconds. This difference is due to the configuration of the PA direction which provides a more direct neutron path to the tumor target, resulting in a much higher dose rate on the GTV. Meanwhile, the LLAT direction experiences greater neutron scattering

because it has to pass through more lateral tissue, so the dose rate is lower and the time required is longer.

In addition, it can be seen that the higher the boron concentration, the more the irradiation time tends to decrease. From the PA direction, increasing the concentration from 100 μg/g to 145 μg/g decreased the irradiation time from 308.48 seconds to 259.43 seconds. A similar effect occurred for the LLAT direction, decreasing the time from 4726.13 seconds to 2955.57 seconds. This is in accordance with the theory that increasing the boron concentration will increase the chance of a reaction $^{10}B(n,\alpha)^{7}Li$, thereby accelerating the accumulation of therapeutic doses in the target.

In this study, dose distributions are presented primarily as organ-averaged equivalent doses and irradiation times. Although bar charts effectively summarize the relative contributions of different irradiation geometries, a more comprehensive visualization such as dose–volume histograms (DVHs) or isodose contour maps would provide additional insight into spatial dose gradients and target coverage. These advanced visualizations were not included due to limitations of the available PHITS output and computational resources, but are recommended for future BNCT planning studies.

Another limitation is the absence of clinical BNCT data for ovarian cancer, which restricts direct validation of the present simulation results. Nevertheless, preclinical evidence indicates the feasibility of BNCT in this context. Recent preclinical work by Laird et al. showed that BSH-BPMO nanoparticles achieved approximately 50-fold higher boron uptake in OVCAR8 ovarian cancer cells compared to free BSH after 24 hours, highlighting the potential of nanoparticle carriers to enhance boron accumulation in ovarian tumor cells [42]. These findings support the rationale for future translational studies, including in vivo validation and pharmacokinetic characterization in ovarian cancer models.

5. CONCLUSION

This study demonstrated the feasibility of BNCT dose simulation for ovarian cancer oligometastases using PHITS v3.35. Among the tested irradiation geometries and boron concentrations, the posterior–anterior (PA) beam with 120 μg/g boron concentration provided the most favorable balance between tumor coverage and organ-at-risk sparing. While these findings are promising, they represent an idealized simulation scenario and should not be directly extrapolated to clinical practice. Further validation with voxel-based dose evaluation, experimental studies, and patient-specific pharmacokinetic data will be required before BNCT can be considered as a viable treatment option for ovarian cancer.

ACKNOWLEDGMENT

Thanks to several parties who have been involved in the research and preparation of the journal, including:

1. JAEA for providing the infrastructure for researchers to simulate radiotherapy through the PHITS software.
2. National Research and Innovation Agency (BRIN), which organizes the activity of internship MBKM.
3. Maulana Malik Ibrahim Islamic State University Malang for their knowledge and advice during this research project.

REFERENCES

1. World Health Organization, “Cancer.” Accessed: Aug. 20, 2025. [Online]. Available: https://www.who.int/health-topics/cancer#tab=tab_1
2. Ferlay J., *et al.*, “Cancer Statistics for the Year 2020: An Overview,” *Int. J. Cancer*, vol. 149, no. 4, pp. 778–789, 2021, doi: 10.1002/ijc.33588.
3. Prihantono, Rusli R., Christeven R., and Faruk M. “Cancer Incidence and Mortality in a Tertiary Hospital in Indonesia: An 18-Year Data Review,” *Ethiop. J. Health Sci.*, vol. 33, no. 3, pp. 515–522, 2023, doi: 10.4314/ejhs.v33i3.15.
4. Javadi S., Ganeshan D., M., Qayyum A., Iyer R., B., and Bhosale P. “Ovarian Cancer, the Revised FIGO Staging System, and the Role of Imaging,” *Am. J. Roentgenol.*, vol. 206, no. 6, pp. 1351–1360, 2016, doi: 10.2214/AJR.15.15199.
5. Xiao L., Li H., and Jin Y., “Automated Early Ovarian Cancer Detection System Based on Bioinformatics,” *Sci. Rep.*, vol. 14, no. 1, p. 22887, 2024, doi: 10.1038/s41598-024-71863-9.
6. Wang L., *et al.*, “TMTP1-modified Polymeric Micelles for the Inhibition of Ovarian Cancer Metastasis and Recurrence through Enhanced Photothermal-immunotherapy,” *Mater. Today Bio*, vol. 32, no. February, p. 101825, 2025, doi: 10.1016/j.mtbio.2025.101825.
7. Le Saux O., I. Ray-Coquard, and S. I. Labidi-Galy, “Challenges for immunotherapy for the treatment of platinum-resistant ovarian cancer,” *Semin. Cancer Biol.*, vol. 77, no. May 2020, pp. 127–143, 2021, doi: 10.1016/j.semcancer.2020.08.017.
8. Kowalchuk R., O., *et al.*, “Stereotactic Body

Radiation Therapy in the Treatment of Ovarian Cancer," *Radiat. Oncol.*, vol. 15, no. 1, pp. 1–10, 2020, doi: 10.1186/s13014-020-01564-w.
9. He H., *et al.*, "The Basis and Advances in Clinical Application of Boron Neutron Capture Therapy," *Radiat. Oncol.*, vol. 16, no. 1, pp. 1–8, 2021, doi: 10.1186/s13014-021-01939-7.
10. Hirose K., *et al.*, "Boron Neutron Capture Therapy using Cyclotron-based Epithermal Neutron Source and Borofalan (10B) for Recurrent or Locally Advanced Head and Neck Cancer (JHN002): An Open-label Phase II Trial," *Radiother. Oncol.*, vol. 155, pp. 182–187, 2021, doi: 10.1016/j.radonc.2020.11.001.
11. Papulino C., *et al.*, "'Aging and Epigenetic Implications in Radiotherapy: The Promise of BNCT,'" *Ageing Res. Rev.*, vol. 110, no. May, p. 102786, 2025, doi: 10.1016/j.arr.2025.102786.
12. Toptas T., Pestereli E., Erol O., Bozkurt S., Erdogan G., and Simsek T., "Validation of Revised FIGO Staging Classification for Cancer of the Ovary, Fallopian Tube, and Peritoneum Based on a Single Histological Type," *Int. J. Gynecol. Cancer*, vol. 26, no. 6, pp. 1012–1019, 2016, doi: 10.1097/IGC.0000000000000736.
13. Miyatake S., I., Wanibuchi M., Hu N., and Ono K., "Boron Neutron Capture Therapy for Malignant Brain Tumors," *J. Neurooncol.*, vol. 149, no. 1, pp. 1–11, 2020, doi: 10.1007/s11060-020-03586-6.
14. Hu K., *et al.*, "Boron Agents Nneutron Capture Therapy," *Coord. Chem. Rev.*, vol. 405, p. 213139, 2020, doi: 10.1016/j.ccr.2019.213139.
15. Hiratsuka J., *et al.*, "Boron Neutron Capture Therapy for vulvar Melanoma and Genital Extramammary Paget's Disease with Curative Responses," *Cancer Commun.*, vol. 38, no. 1, pp. 1–10, 2018, doi: 10.1186/S40880-018-0297-9.
16. Green S., *et al.*, "Accelerator Neutron Sources for BNCT: Current Status and some Pointers for Future Development," *Appl. Radiat. Isot.*, vol. 217, no. November 2024, p. 111656, 2025, doi: 10.1016/j.apradiso.2025.111656.
17. Porras I., *et al.*, "BNCT Research Activities at the Granada Group and the Project NeMeSis: Neutrons for Medicine and Sciences, Towards an Accelerator-based Facility for new BNCT Therapies, Medical Isotope Production and other Scientific Neutron Applications," *Appl. Radiat. Isot.*, vol. 165, no. April, 2020, doi: 10.1016/j.apradiso.2020.109247.
18. Shuto Y., Nakamura S., Imamichi S., and Shimada K., "Relative Biological Effectiveness of an Accelerator-based BNCT System Coupled to a Solid-state Lithium Target : Two Different Approaches for Neutron Beams," *Appl. Radiat. Isot.*, vol. 222, no. February, p. 111834, 2025, doi: 10.1016/j.apradiso.2025.111834.
19. Kato T., *et al.*, "Design and Construction of an Accelerator-based Boron Neutron Capture Therapy (AB-BNCT) Facility with Multiple Treatment Rooms at the Southern Tohoku BNCT Research Center," *Appl. Radiat. Isot.*, vol. 156, no. January 2019, p. 108961, 2020, doi: 10.1016/j.apradiso.2019.108961.
20. Murilla R., M., Edilo G., G., Budlayan M., L., M.,, and Auxtero E., S., "Boron Delivery Agents in BNCT: A Mini Review of Current Developments and Emerging Trends," *Nano TransMed*, vol. 4, no. March, p. 100081, 2025, doi: 10.1016/j.ntm.2025.100081.
21. Zhu Y., Lin Z., Yu H.,, Yu X., and Dai Z. "Conceptional Design of an Adjustable Moderator for BNCT Based on a Neutron Source of 2.8 MeV Proton Bombarding with Li Target," *Nucl. Eng. Technol.*, vol. 56, no. 5, pp. 1813–1821, 2024, doi: 10.1016/j.net.2023.12.038.
22. Purohit M., and Kumar M. "Boron Neutron Capture Therapy: History and Recent Advances," *Mater. Today Proc.*, no. xxxx, 2022, doi: 10.1016/j.matpr.2022.12.181.
23. Ge Y., *et al.*, "Design of a Mixed Material Moderator in a Beam-shaping Assembly for Proton Accelerator-based Boron Neutron Capture Therapy," *Appl. Radiat. Isot.*, vol. 214, no. September, p. 111515, 2024, doi: 10.1016/j.apradiso.2024.111515.
24. Qiu J., *et al.*, "Preliminary Study of a Compact Epithermal Neutron Absolute Flux Intensity Measurement System for Real-time In-vivo Dose Monitoring in Boron Neutron Capture Therapy," *Radiat. Meas.*, vol. 178, no. October, p. 107308, 2024, doi: 10.1016/j.radmeas.2024.107308.
25. Sato T., *et al.*, "Recent Improvements of the particle and heavy ion transport code system–PHITS Version 3.33," *J. Nucl. Sci. Technol.*, vol. 61, no. 1, pp. 127–135, 2024, doi: 10.1080/00223131.2023.2275736.
26. Zhong W., B., Chen J. Teng Y., C., and Y. H. Liu Y., H. "Introduction to the Monte Carlo Dose Engine COMPASS for BNCT," *Sci. Rep.*, vol. 13, no. 1, pp. 1–11, 2023, doi: 10.1038/s41598-023-38648-y.
27. Song H., *et al.*, "Impact of Nuclear Cross-section Libraries on Neutron Beam Quality and Dose Distribution in Accelerator-based BNCT :

a Full-process Monte Carlo Study," *Radiat. Phys. Chem.*, vol. 237, no. May, p. 113099, 2025, doi: 10.1016/j.radphyschem.2025.113099.
28. Carter L., M., *et al.*, "PARaDIM: A PHITS-Based Monte Carlo Tool for Internal Dosimetry with Tetrahedral Mesh Computational Phantoms," *J. Nucl. Med.*, vol. 60, no. 12, pp. 1802–1811, 2019, doi: 10.2967/jnumed.119.229013.
29. Kuga N., Shiiba T., Sato T., Hashimoto S., and Kuroiwa Y., "Experimental and Computational Verifications of the Dose Calculation Accuracy of PHITS for High-energy Photon Beam Therapy," *J. Nucl. Sci. Technol.*, vol. 61, no. 1, pp. 136–145, 2024, doi: 10.1080/00223131.2023.2275737.
30. Ladbury C., *et al.*, "Stereotactic Body Radiation Therapy for Gynecologic Malignancies: A Case-Based Radiosurgery Society Practice Review," *Pract. Radiat. Oncol.*, vol. 14, no. 3, pp. 252–266, 2024, doi: 10.1016/j.prro.2023.09.008.
31. Nakamura R., Hino M., Tanaka H., Kuriyama Y., and Iwashita Y. "Conceptual Design of a Target Station using a 30-MeV Cyclotron Accelerator for the Basic Study of Boron Neutron Capture Therapy at KURNS," *Nucl. Instruments Methods Phys. Res. Sect. A Accel. Spectrometers, Detect. Assoc. Equip.*, vol. 1042, no. August, p. 167425, 2022, doi: 10.1016/j.nima.2022.167425.
32. Ardana I., M., and Sardjono Y, "Optimization of a Neutron Beam Shaping Assembly Design for Bnct and Its Dosimetry Simulation Based on Mcnpx," *J. Teknol. Reakt. Nukl. Tri Dasa Mega*, vol. 19, no. 3, p. 121, 2017, doi: 10.17146/tdm.2017.19.3.3582.
33. Hu N., *et al.*, "Evaluation of PHITS for Microdosimetry in BNCT to Support Radiobiological Research," *Appl. Radiat. Isot.*, vol. 161, no. November 2019, 2020, doi: 10.1016/j.apradiso.2020.109148.
34. Pistone D., *et al.*, "A GATE Monte Carlo Study on ICRP110 Phantoms for BNCT Dosimetry Evaluation," *Appl. Radiat. Isot.*, vol. 220, no. February, p. 111724, 2025, doi: 10.1016/j.apradiso.2025.111724.
35. Lee C., M., and Lee H., S. "Development of a Dose Estimation Code for BNCT with GPU Accelerated Monte Carlo and Collapsed Cone Convolution Method," *Nucl. Eng. Technol.*, vol. 54, no. 5, pp. 1769–1780, 2022, doi: 10.1016/j.net.2021.11.010.
36. Hu N., *et al.*, "Evaluation of a Treatment Planning System Developed for Clinical Boron Neutron Capture Therapy and Validation Against an Independent Monte Carlo Dose Calculation System," *Radiat. Oncol.*, vol. 16, no. 1, 2021, doi: 10.1186/s13014-021-01968-2.
37. Harish A., F., Warsono, and Sardjono Y. "Dose Analysis of Boron Neutron Capture Therapy (BNCT) Treatment for Lung Cancer Based on Particle and Heavy Ion Transport Code System (PHITS)," *ASEAN J. Sci. Technol. Dev.*, vol. 35, no. 3, pp. 187–194, 2020, doi: 10.29037/ajstd.545.
38. Sato T, Furuta T., Sasaki H., and Watabe T. "Establishment of a Practical Methodology for Evaluating Equieffective Dose of Individual Patients Based on RT-PHITS," *EJNMMI Phys.*, vol. 12, no. 1, 2025, doi: 10.1186/s40658-025-00743-6.
39. Moghaddasi L., and Bezak E. "Development of an Integrated Monte Carlo Model for Glioblastoma Multiforme Treated with Boron Neutron Capture Therapy," *Sci. Rep.*, vol. 7, no. 1, pp. 1–14, 2017, doi: 10.1038/s41598-017-07302-9.
40. Komori S., *et al.*, "Dosimetric Effect of Set-up Error in Accelerator-based Boron Neutron Capture Therapy for Head and Neck Cancer," *J. Radiat. Res.*, vol. 63, no. 4, pp. 684–695, 2022, doi: 10.1093/jrr/rrac017.
41. Tang F., *et al.*, "Evaluation of Pharmacokinetics of Boronophenylalanine and Its Uptakes in Gastric Cancer," *Front. Oncol.*, vol. 12, no. July, pp. 1–11, 2022, doi: 10.3389/fonc.2022.925671.
42. Laird M., *et al.*, "Organosilica Nanoparticles Containing Sodium Borocaptate (BSH) Provide New Prospects for Boron Neutron Capture Therapy (BNCT): Efficient Cellular Uptake and Enhanced BNCT Efficacy," *Nanoscale Adv.*, vol. 5, no. 9, pp. 2537–2546, 2023, doi: 10.1039/d2na00839d.

APPENDIX